Supplementary Figures

Figure S1 CD11b+ myeloid cells are required for oncogenic Kras driven PanIN formation. (A) Percentage of CD11b+CD64+F4/80+ macrophages in wild--type control, iKras* and iKras*;;CD11b--DTR pancreata measured by flow cytometry one week post pancreatitis induction. Data represent mean ± SEM, each point indicates one mouse (n=3--5). The statistical difference was determined by two--tailed Student's t--tests. (B) Co--immunofluorescent staining for Amylase (red), CK19 (green) and DAPI (blue) in wild--type control, CD11b--DTR, iKras* and iKras*;;CD11b--DTR pancreata. Scale bar 25μm. (C) Periodic acid–Schiff (PAS) staining of wild--type control, CD11b--DTR, iKras* and iKras*;;CD11b--DTR pancreata 1 week post pancreatitis induction. Scale bar 50μm. (D) Quantification of p--ERK1/2 positive areas per high power field (400X). Data represent mean ± SEM. Statistical difference was determined by two--tailed Student's t--tests.

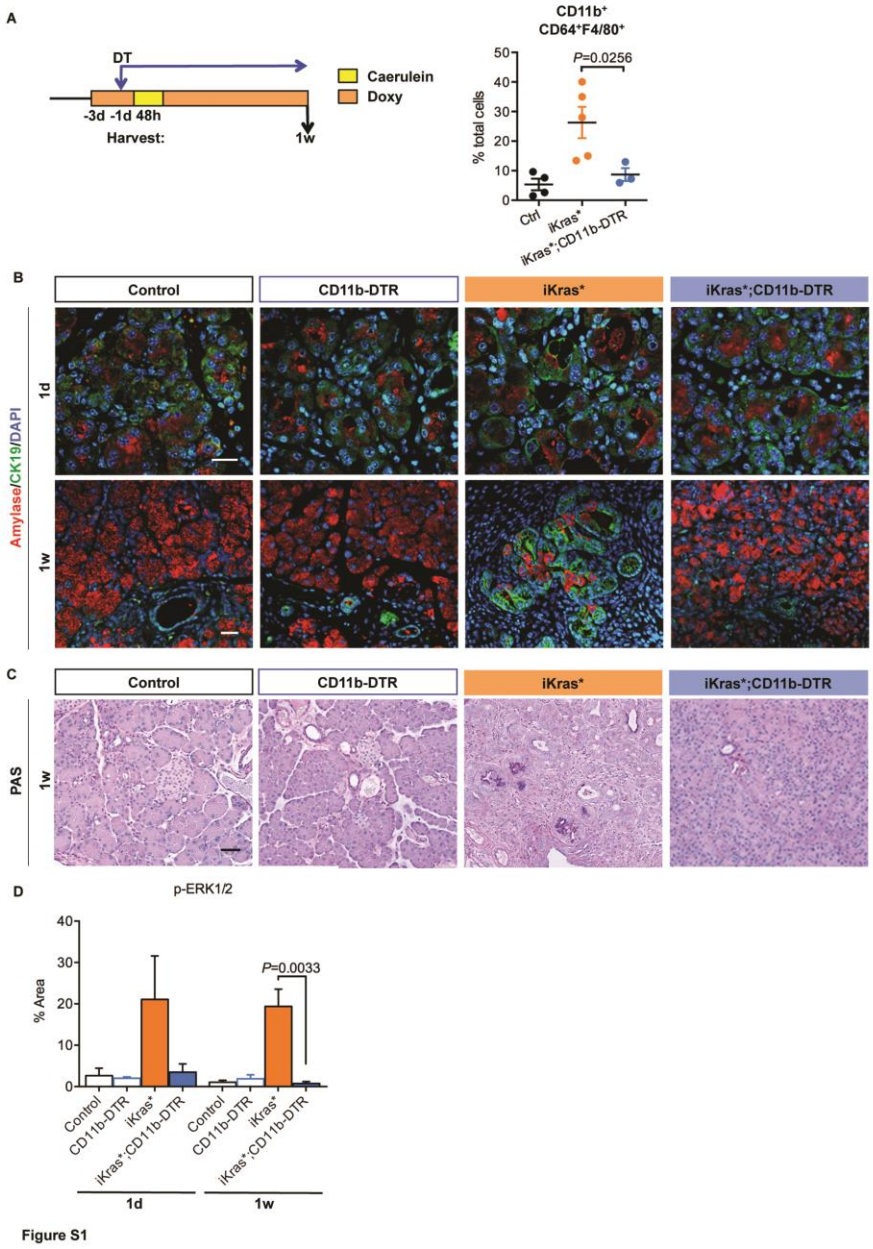

Figure S1

Figure S2 DT treatment reduces subcutaneous tumor progression in CD11b--DTR mice by inducing cell apoptosis. (A) Experimental design. (B) Immunohistochemistry for F4/80 in control and DT treated subcutaneous iKras* tumors. Scale bar 50µm. Graph depicts the quantification of F4/80+ areas per high power field (200X). Data represent mean ± SEM, 3 HPF for each mouse. Statistical difference was determined by two--tailed Student's t--tests. (C)Immunohistochemistry for Ki67 and (D) TUNEL staining in subcutaneous tumors dissected from the control and DT treated CD11b--DTR mice. Scale bar 50µm.

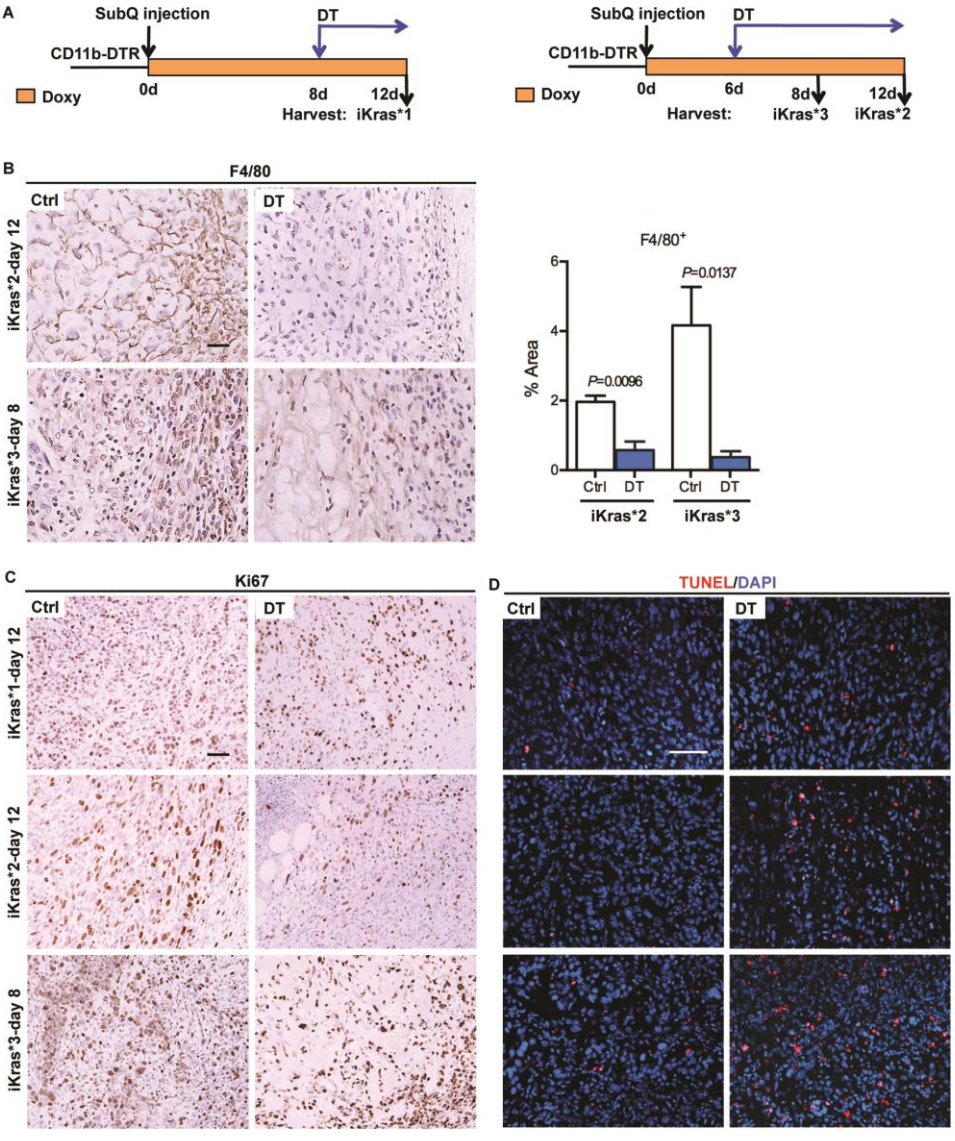

Figure S2

Figure S3 DT treatment depletes macrophages and enhances tumor--infiltrating CD8+ T cells. (A) qRT--PCR for the macrophage markers Agr1, Msr1 and Mrc1 expression in control and DT treated subcutaneous tumors. Data represent mean ± SEM, each point indicates one sample (n=5--7). The statistical difference was determined by two--tailed Student's t--test. (B) Co--immunofluorescent staining for CD8 (red), GFP (indicating tumor cells, green) and DAPI (blue) in control and DT treated iKras*3 subcutaneous tumors. Scale bar 50μm. Red arrows point to CD8+ T cells. White dash line indicates the boundary of the tumor. (C) Percentage of CD3+CD4+CD25+Foxp3+ Treg cells in control and DT treated iKras*3 subcutaneous tumors measured by flow cytometry. Data represent mean ± SEM, each point indicates one tumor (n=4). The statistical difference was determined by Student's t--tests. *p<0.05. (D) qRT--PCR for Pdcdlg1 and Pdcdlg2 expression in flow sorted CD45+CD11b+F4/80+ macrophages;; (E) qRT--PCR for Pdcdlg1, Ctla4, Il2 and Ifn??expression in flow sorted CD3+CD8+ T cells. Data represent mean ± SEM, n=3. The statistical difference was determined by two--tailed Student's t--test.

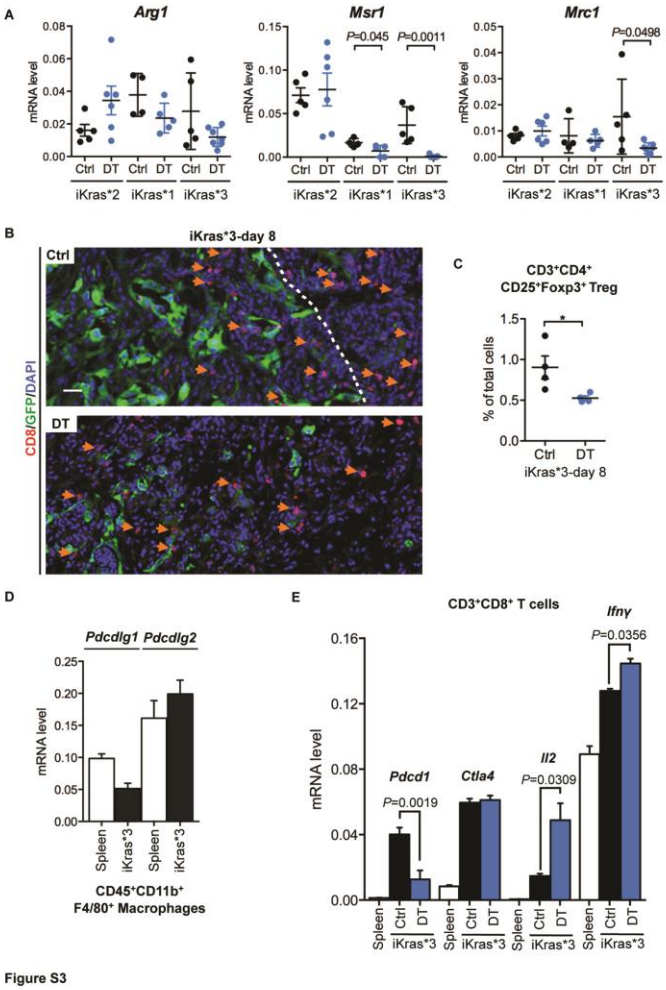

Figure S3

Figure S4 PD--1 blockade has limited efficacy in pancreatic cancer. (A) Experimental design and tumor size change of subcutaneous iKras* tumors following short--term lgG or anti--PD--1 treatment. Data represent mean ± SEM, n=5--8. Statistical difference was analyzed by Two--Way ANOVA. (B) Co--immunofluorescent staining for CD8 (red), GFP (tumor cells, green), CD3 (grey) and DAPI (blue) in control and anti--PD--1 treated subcutaneous iKras*1 and iKras*3 tumors. Scale bar 25μm. Graph depicts the quantification of CD3+CD8+ cell number per high power field (400X). Data represent mean ± SEM, 3 HPF for each mouse. Statistical difference was determined by two--tailed Student's t--tests. (C) qRT--PCR for the CD8+ T cell activation markers Ifn?, Ifn?1, Prf--1 and Gzmb expression in control and anti--PD--1 treated subcutaneous tumors. Data represent mean ± SEM, each point indicates one sample (n=5--6). The statistical difference was determined by two--tailed Student's t--test. (D) Experimental design and tumor size change (%) of subcutaneous 7940B tumors post lgG or anti--PD--1 treatment. (E) qRT--PCR for Ctla4 expression in control and anti--PD--1 treated subcutaneous iKras* tumors. Data represent mean ± SEM, each point indicates one sample (n=4--5). The statistical difference was determined by two--tailed Student's t--test. (F) Pdcdlg1 expression in GFP+CD11b-- iKras*1, iKras*2 and iKras*3 cells that flow sorted from subcutaneous tumors and following culturing in vitro for 2 days after sorting. Data represent mean ± SEM.

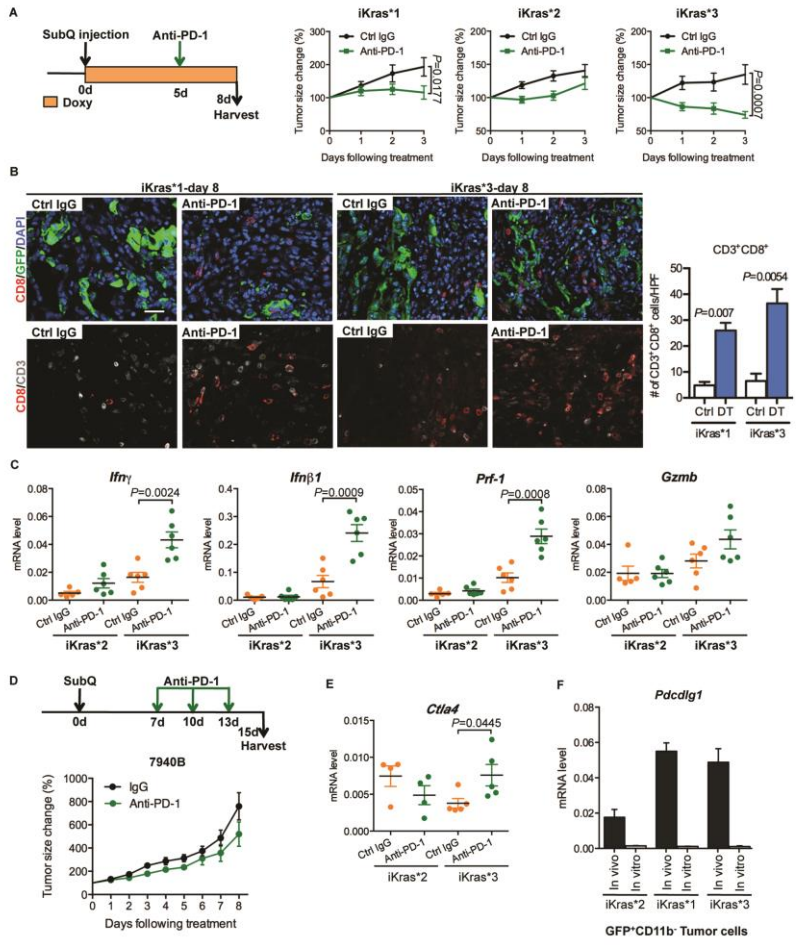

Figure S4

Figure S5 TAMs, T cells and bone marrow derived cells induce PD--L1 expression in pancreatic cancer cells in vitro. (A) Left: co--culture model of iKras*3 cells with TAMs or T cells flow sorted from iKras*3 subcutaneous tumors. Right: qRT--PCR for Pdcdlg1 expression in iKras*3 cells alone or co--cultured with tumor associated immune cells. Data represent mean ± SEM, n=3. The statistical difference was determined by two--tailed Student's t--test. (B) qRT--PCR for PDCDLG1 and PDCDLG2 expression in human PDA cells alone or co--cultured with murine bone marrow derived cells. Data represent mean ± SEM, n=3. The statistical difference was determined by two--tailed Student's t--tests. (C) qRT--PCR for F4/80, iNos2, Arg1, Msr1 and Mrc1 expression in murine bone marrow derived cells alone or co--cultured with human PDA cells. Data represent mean ± SEM.

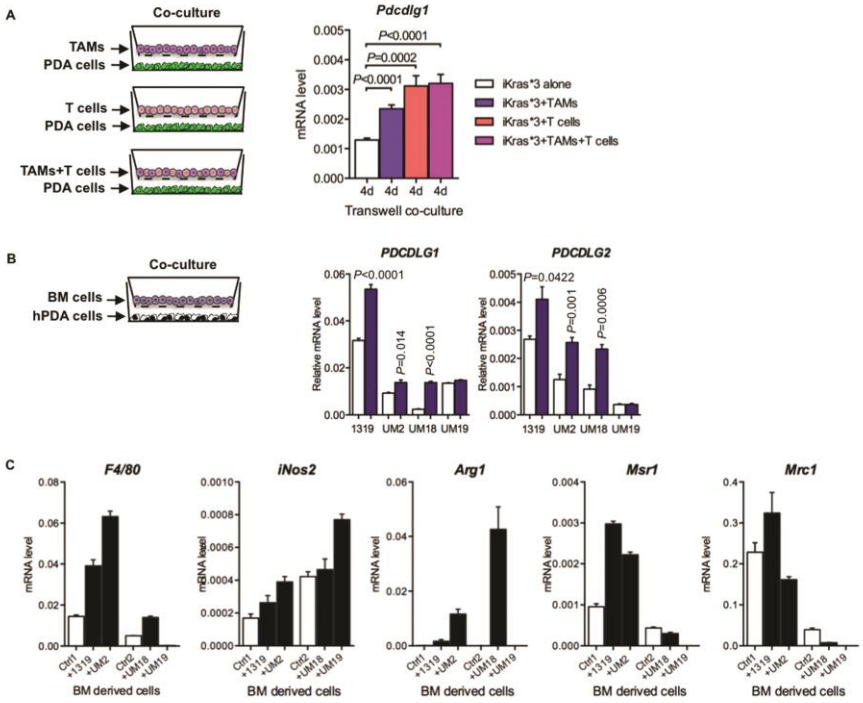

Figure S5

Figure S6 IL6/Stat3 signaling is not involved in myeloid cell induced PD--L1 regulation. (A)Experimental design. (B) Western blotting for MAPK, IL6 signaling components and PD--L1 in human PDA cells alone, co--cultured with BM cells and followed by vehicle, MEKi or anti--IL6 treatment. (C) qRT--PCR for PDCDLG1 and (D) IL6 expression in human PDA cells alone, co--cultured with BM cells and followed by vehicle, MEKi or anti--IL6 treatment. Data represent mean ± SEM, n=3. The statistical difference was determined by two--tailed Student's t--test. (E) Experimental design. (F) Western blotting for MAPK, IL6 signaling components and PD--L1 levels, and qRT--PCR for PDCDLG1 expression in vehicle control or recombinant human IL6 treated UM2 cells. Data represent mean ± SEM.

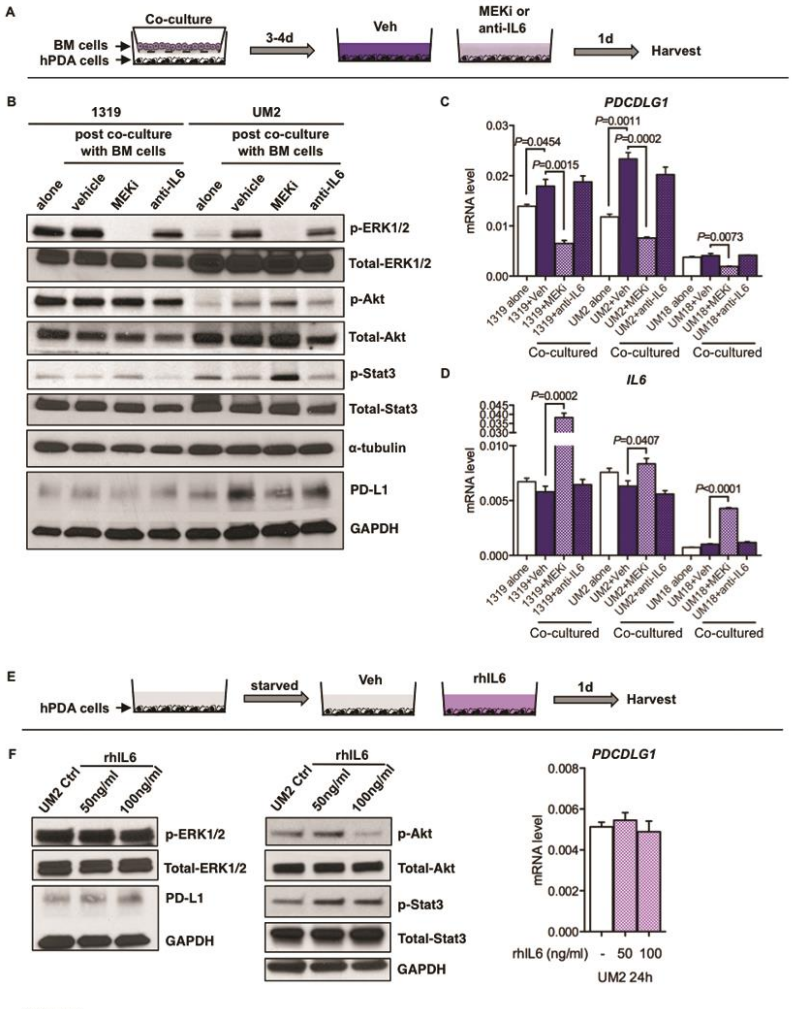

Figure S6